(ii) Errors due to number of cameras

Ideally, all cameras see each marker at every point in time. In real situations, this is not the case, and markers are lost from view. In film analysis, the positions of these lost markers may be determined using a best estimate based on the position of the body. In video analysis, these markers are lost until they are once again visible to the camera. The position of a marker at a given point in time is calculated using only those cameras that see the marker. This may be critical for certain camera placements and camera numbers.

As an example, an experiment is performed using three cameras: 1, 2, and 3. Assume that the optical axes of cameras 1 and 2 intersect at an angle of 90°, and the optical axes of cameras 1 and 3 intersect with an angle of 20°. At time, t_1, the position of marker, k, is determined using information from all three cameras. At time, t_2, information from camera 2 is missing. At time, t_3, information from all three cameras is again available. The results for this example are illustrated for the x and y coordinates in Figure 3.6.4.

For instance, frames 15 and 19 use (for three different norm of residuals) a different number of cameras than do frames 16, 17, and 18, (which all use the same number of cameras) to determine the position of marker, k.

Obviously, a change from six to five cameras would induce less change in the final coordinate calculation than a change from three to two cameras. In general, noise in coordinates decreases with an increasing number of cameras. However, this is not necessarily equivalent to an increase in accuracy of the determined marker positions.

(iii) Errors due to calibration

The accuracy of the measured data depends considerably on the accuracy of the calibration procedure. It is often assumed that accuracy increases the more the calibrated volume fills the field of view. However, the situation is more complex than this assumption. Lenses are not ideal structures, and have errors that influence the accuracy of the collected data. Consequently, data should be corrected for lens errors. Several software packages do this, as described above. If data is not corrected for lens errors, calibration of the central part of the field of view, where the lens usually has fewer errors than at its boundaries, may be better than using calibration frames that exploit the entire field of view. Additionally, errors in determining the position of markers depend on the accuracy of the calibration marker setup. Errors in the location of these markers affect the accuracy of marker coordinates.

However, most current commercial camera systems offer calibration procedures and software that reduce calibration errors substantially. The most elegant and effective calibration method uses a calibration rod, which is moved in the calibration space and covers the whole calibration volume. This calibration rod provides data to achieve excellent calibration results.

(iv) Errors due to digitization

Conventional film analysis typically uses manual digitization. Results from manual digitization may be affected by:

- Random inaccuracies of the digitizing operator in positioning the digitization pen. Such errors can be reduced by employing appropriate marker shapes (spherical), markers with dots in the middle, and multiple digitization, and
- Placement of cameras (see above).

Video analysis often uses automatic digitization. The accuracy of automatic digitization depends on various factors such as:

- Number of cameras (see above),
- Placement of cameras (see above),
- Marker shape (spherical markers are typically used because they have the same shape irrespective of the direction from which they are viewed),
- Size of the markers (the centroid can be determined with better accuracy for a large than for a small marker),
- Merging of markers (the centroid of a marker cannot be correctly established),
- Partial cover of a marker (the centroid of a marker cannot be correctly established), and
- Threshold level of the video system (determines how well the video screen estimates the spherical image of the marker).

Most of these problems can be solved with appropriate preparations of the setup and adequate software.

3.6.3 DETERMINING RIGID BODY KINEMATICS

The three-dimensional marker positions are used to determine limb segment positions and orientations. This process, and associated errors, are discussed in the first two parts of this section. Position and orientation of the limb segments can be used to describe the relative orientation and movement of limb segments. Methods used to describe relative limb segment orientations commonly used in biomechanics are discussed in the balance of this section

RECONSTRUCTION OF RIGID BODY MOTION FROM MARKER POSITIONS

Marker based coordinate systems

A coordinate system is defined for each limb segment or body of interest (Figure 3.6.7). Limb segments are often assumed to be a rigid body. Thus, if the position and orientation of the segment fixed coordinate system is known, then the position of any point on the limb

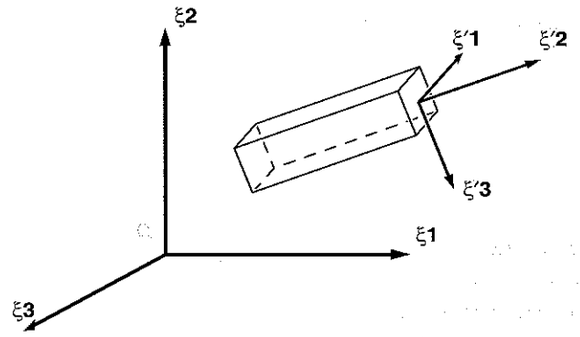

Figure 3.6.7 **Orientation of a rigid body in space with an embedded Cartesian coordinate system, ξ', relative to a reference Cartesian coordinate system, ξ.**

segment is known. Since the positions of the optical markers are measured, it is easiest to define the segment fixed coordinate system based on the markers that are attached to that segment. This can be done with three or more than three markers:

(i) Using three markers to determine a coordinate system

Three markers is the minimum number required to completely define a coordinate system. An example of how a segment coordinate system can be defined for a segment of interest is outlined below. Assume:

A	=	first marker on the segment of interest
B	=	second marker on the segment of interest
C	=	third marker on the segment of interest
$\mathbf{a}$	=	position vector of point A in the lab coordinate system
$\mathbf{b}$	=	position vector of point B in the lab coordinate system
$\mathbf{c}$	=	position vector of point C in the lab coordinate system
$\xi'\mathbf{1}$	=	direction vector of the first axis of the segment coordinate system
$\xi'\mathbf{2}$	=	direction vector of the second axis of the segment coordinate system
$\xi'\mathbf{3}$	=	direction vector of the third axis of the segment coordinate system

Any point can be used as the origin, O, of the segment coordinate system. Assume that the point A has been selected to be the origin. For this assumption, the unit vector $\xi'\mathbf{1}$ representing the direction of the first axis can be defined as the direction vector from point A to point B:

$$\xi'\mathbf{1} = \frac{\mathbf{b}-\mathbf{a}}{|\mathbf{b}-\mathbf{a}|}$$

The unit vector $\xi'\mathbf{3}$, representing the direction of the third axis can be defined as the cross-product between the unit vector $\xi'\mathbf{1}$ and the unit vector pointing from A to C:

$$\xi'\mathbf{3} = \xi'\mathbf{1} \times \frac{\mathbf{c}-\mathbf{a}}{|\mathbf{c}-\mathbf{a}|}$$

The unit vector $\xi'2$, representing the direction of the second axis can then be defined as the cross product of the unit vectors $\xi'\mathbf{3}$ and $\xi'\mathbf{1}$:

$$\xi'2 = \xi'\mathbf{3} \times \xi'\mathbf{1}$$

In this arbitrary example, the unit vectors $\xi'\mathbf{1}$, $\xi'\mathbf{2}$ and $\xi'\mathbf{3}$ are the bases vectors of the limb fixed coordinate system. They determine position and orientation of the segment of interest.

(ii) Using more than three markers to determine a coordinate system

If there were no errors in the marker positions, and the limb segment was truly a rigid body, then additional markers beyond the required three would be of no use. However, since limb segments may not be truly rigid, and there may be errors in marker positions, additional markers may improve the accuracy of limb segment position and orientation reconstructions. A least squares method (Veldpaus et al., 1988) or similar method (Söderquist & Wedin, 1993) can be used to determine the segment position and orientation from the marker positions.

These methods are relatively sophisticated algorithms, but simply described, they do the following. Given the positions of the markers fixed to some segment at two different times (or positions of the segment of interest), the displacement and rotation of that segment that occur between these two points of time are determined that minimize the sum:

$$\min \sum_{k=1}^{n} \left(|\mathbf{m}_{ki} - (\mathbf{d}_{ij} + R_{ij}\mathbf{m}_{kj})|\right)$$

where:

$\mathbf{m}_{ki}$	=	position vector of marker k at time i
$\mathbf{m}_{kj}$	=	position vector of marker k at time j
n	=	total number of markers
R_{ij}	=	rotation that occurs from time i to time j
$\mathbf{d}_{ij}$	=	position vector of point A in the lab coordinate system

Thus, the displacement and rotation are selected that move the markers at time i so that they lie as close as possible to the markers at time j. By using these optimization methods, inaccuracies in the position description caused by changes in the relative marker positions due to deformation of the body are averaged over the whole time interval of data collection.

Anatomically significant coordinate systems

The selection or definition of a coordinate system fixed to a specific segment is an important step. Usually, the coordinate system is defined such that each of the coordinate directions has some anatomical significance. It is common, for example, for the coordinate system to be aligned with the anatomical coordinate system so that when movements or displacements are measured, they can be described in clinically relevant terms.

However, markers often cannot be located on limb segments in positions appropriate for the definition of an anatomically significant coordinate system. In such cases, it is often easiest to define the orientation of the limb segment fixed coordinate system using a neutral position.

The use of a neutral position consists of positioning the subject in a neutral or reference position (often the anatomical position). Measurements are then made to determine the marker positions relative to the selected anatomically significant coordinate system. The coordinate system fixed to the limb segment does not need to be explicitly constructed from the locations of the markers. The positions measured during the neutral trial can then be compared to the measured positions during the movement of interest to determine absolute position and orientation of the anatomically relevant limb segment fixed coordinate system.

The comparison of the measured marker positions to the neutral position marker positions can be done using the methods developed for using three or more markers to track a body described above. The least squares method (Veldpaus et al., 1988) or singular value decomposition method of Söderquist and Wedin (1993) can be used in the following way for 3 or more markers:

${}^{L}\mathbf{m}_1, {}^{L}\mathbf{m}_2, \ldots {}^{L}\mathbf{m}_n$	position vectors of markers 1 through n, expressed relative to the anatomically significant limb segment fixed coordinate system L (measured using a neutral position)
${}^{A}\mathbf{m}_{1i}, {}^{A}\mathbf{m}_{2i}, \ldots {}^{A}\mathbf{m}_{ni}$	position vectors of markers 1 through n at time i, expressed relative to the absolute coordinate system A

Output:

$\mathbf{d}_i$	the displacement of the limb segment fixed coordinate system relative to the absolute coordinate system at time i
R_i	the orientation of the limb segment fixed coordinate system relative to the absolute coordinate system at time i

This method produces similar results to the rigid body reconstruction method using an explicit definition of the coordinate system in terms of marker positions with the two following advantages:

- The limb segment fixed coordinate system can be defined in a convenient way using a neutral position, and
- Three or more markers can be used in an optimal way to minimize errors caused by errors in the marker data or non-rigidity of the limb segment.

ERRORS IN RIGID BODY MOTION USING MARKER INFORMATION

Markers attached to a segment of interest may not always represent true skeletal locations. These differences are referred to as relative and absolute errors. The placement of the markers can also substantially influence the propagation of marker coordinate errors and relative marker movement errors when calculating segment kinematics:

Relative marker error is the relative movement of two markers with respect to each other.
Comment: the relative marker error establishes how well the markers on the segment estimate the rigid body assumption. This error is caused by soft tissue movement.

Absolute marker error is the movement of one specific marker with respect to specific bony landmarks of a segment.
Comment: this error establishes the actual accuracy of the measurement.

(i) Errors due to relative marker movement

The three-dimensional motion of body segments is typically described using rigid body mechanics. The spatial coordinates of segment landmarks are used directly or indirectly to

define body-fixed coordinate systems for each segment. Markers placed on the skin of a subject or animal are assumed to represent the location of bony landmarks of the segment of interest. However, skin movement and movement of underlying bony structures are not necessarily identical, and substantial errors may be introduced in the description of bone movement when using skin-mounted marker arrays (Lesh et al., 1979; Ladin et al., 1990). Three major approaches have been suggested to correct skin displacement errors: invasive marker placement, data treatment, and marker attachment systems.

Invasive methods provide the most accurate results for bone movement. Bone pins have been used to assess movement of the tibia and femur, e.g., Levens et al. (1948). Knee joint kinematics have been compared for data collected from skin-mounted markers and markers attached to bone pins (Ladin et al., 1990). The results for both methods showed differences of up to 50% for the knee angle. Results from invasive methods are, however, not applicable in most research and clinical settings for movement analysis. Therefore, other approaches are needed.

Mathematical algorithms have been proposed for error reduction in raw data, including skin displacement effects (Plagenhoef, 1968; Miller & Nelson, 1973; Winter et al., 1974; Zernicke et al., 1976; Soudan & Dierckx, 1979; Woltring, 1985; Veldpaus et al., 1988). Smoothing algorithms are based on the assumption that the noise is additive and random with a zero mean value (Woltring, 1985). However, errors due to skin displacement may not have zero means. Mathematical algorithms, as currently used, do not seem to be appropriate approaches for solving the errors due to marker movement relative to bony landmarks.

Marker attachment systems (frames) have recently been developed to reduce errors due to relative marker movement. The following discussion concentrates on the tibia. However, it may be used in analogy for other segments of human or animal bodies. Positional data from four different lightweight marker attachment systems (frames) were compared to data from skin-mounted markers. Frame 1 was constructed from thermoplastic material, frame 2 of rectangular aluminum rods, frame 3 of plastic material of medium stiffness, and frame 4 used laminated plastic strips. The fifth marker attachment system was the attachment of the markers to the skin. Skin displacement errors were analyzed in terms of relative and absolute errors.

The *relative* error was determined as the change in three-dimensional length, ΔL_{ik}, between any two markers with respect to the static length, where:

$$\Delta L_{ik} = L_{ik}^{stat} - L_{ik}^{dyn}$$

and:

$$L_{ik} = \sqrt{(x_i - x_k)^2 + (y_i - y_k)^2 + (z_i - z_k)^2}$$

where:

x_i, y_i, z_i	=	coordinates of marker, i, at the time, t
x_k, y_k, z_k	=	coordinates of marker, k, at the time, t

The results for the relative errors are illustrated in Figure 3.6.8. Marker 1 was mounted close to the distal anterior part of the tibia and marker 2 at the proximal anterior part of the tibia. The four frames substantially reduced the relative movement of marker 1 with respect

to marker 2 when compared to the results for the skin-mounted markers. The biggest length difference during stance between markers 1 and 2 was more than 3 cm in this example. Such differences in length (as measured for the skin-mounted markers) of a structure, which is assumed to be rigid, interfere with the accuracy of the results. These results suggest that markers attached to frames may fulfil the requirements of a rigid body, and that markers attached directly to the skin may not fulfil these conditions satisfactorily.

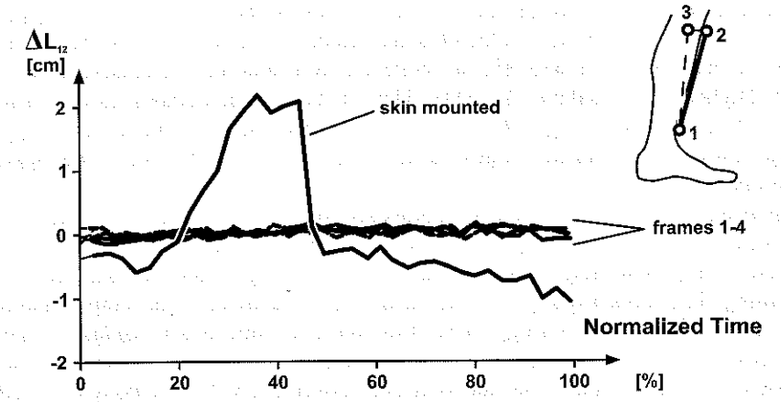

Figure 3.6.8 **Actual three-dimensional length between the markers 1 and 2 during ground contact in running (time 0 corresponds to heel strike, time 100% to take off) for four marker frames and for skin-mounted markers. The graph illustrates results for one subject and is representative of the general trend.**

The use of an array of more than three markers may help solve for relative marker movement. In this case, the distance between all markers is monitored and the markers with the minimal changes in distance, for instance, are used for further calculation.

(ii) Errors due to absolute marker movement

Markers used to determine segmental movement are typically attached to the skin of test subjects. However, there may be relative movement between skin and the underlying bone, especially when high inertia forces are present, e.g., during impact in running, or when high changes in muscle activity occur. Relative movement between skin and bone-mounted markers in dynamic situations has been determined in a few invasive experimental studies (Murphy, 1990; Angeloni et al., 1993; Holden et al., 1994; Lafortune et al., 1994; Andriacchi & Toney, 1995; Capozzo et al., 1996; Reinschmidt, 1996; Reinschmidt et al., 1997a). The agreement between skin and bone marker based kinematics in walking and running ranged from good to virtually no agreement (Reinschmidt et al., 1997b). The difference between the absolute skin marker position and the skeletal marker position was relatively small for the leg, but substantial for the foot/shoe and for the thigh (Figure 3.6.9). The results indicated that skin or shoe markers overestimated the actual bone movement.

(iii) Errors due to inadequate placement of the markers

The placement of the markers on the segment of interest may be a further source of error in determining marker coordinates. Possible factors include:

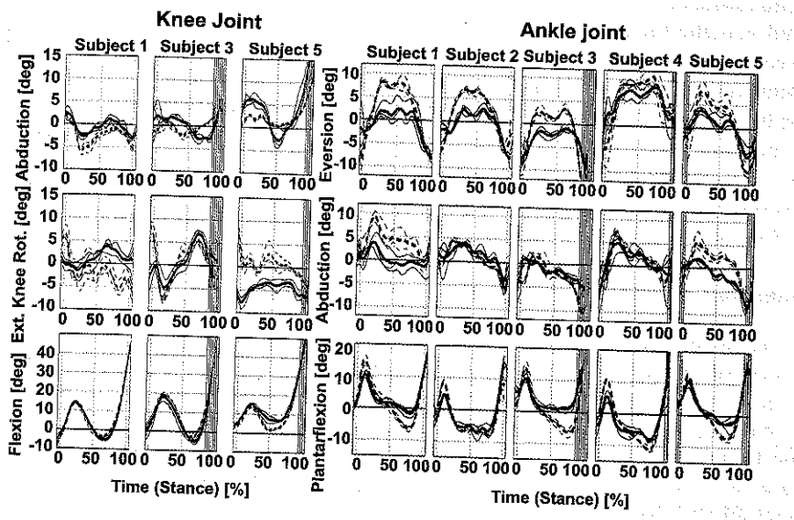

Figure 3.6.9 **Illustration of the positional differences between shin and skeletal muscles for the calcaneus (heel of the shoe), tibia, and femur. The results for the ankle joint are on the left. The results for the knee joint are on the right. Shaded areas at the beginning and end are areas associated with high measuring errors (from Reinschmidt et al., 1997b, with permission).**

- Co-linearity (the markers should define a plane and should not be on one line),
- Distance between markers (large distances between markers improve accuracy), and
- Marker distribution with respect to the axis of rotation of the segment (helical axes are most accurately determined when the helical axis passes directly through the centroid of the marker distribution).

Most of these factors can be controlled with a careful preparation of each segment of interest (Söderquist & Wedin, 1993).

NEW DEVELOPMENTS

In recent years, markerless movement analysis started to emerge. This technique does not rely on optical markers to identify motion variables. This new technique provides total independence from any sort of marking devices. There are two different approaches used in markerless analysis:

Model-based markerless capture

The model based markerless capture uses the same image capture devices as the marker-based method. However, the image processing algorithm is usually very complex, e.g., sil-

houette estimation and matching, and is done successive steps. First, the silhouette is extracted from the background. Second, the picture is segmented, and third, a correspondence between a chosen model of motion and the extracted silhouette is established, usually using an iterative closest point (ICP) algorithm. The method is semi-automatic and often imposes some limits on the complexity of movement that can be reliably traced.

The main disadvantage of this method is that the quality of the results depends on the right choice of a predetermined model of motion, which sometimes proves to be difficult. However, this method has proved to be as reliable as any of the marker-based methods, with the obvious advantage of not depending on markers and marker-related errors.

Model-free markerless capture

The model free markerless capture is completely independent of the subject or the type of motion under scrutiny. The method is still in its infancy and some technical aspects must still be solved. There are no differences between this method and the methods presented above at the hardware level. Furthermore, the image analysis algorithms are almost the same as described earlier. However, this method uses some additional mathematical algorithms that can automatically identify different body moving parts by fitting primitive shapes into a three-dimensional shape. The most common fitting technique uses multiple superquadric shapes to decompose three-dimensional point data into primitive sub-shapes using neural networks, fuzzi clustering cuts and other methods.

A combination of a marker-based and a markerless system has been presented recently (Mündermann et al., 2005). This method identifies body segments using a full body laser scan with markers positioned at the subject (a kind of a calibration). For the actual movement to be studied, the algorithms used to isolate the body from the background are no different from the other markerless methods. The experimental results obtained with this method were comparable with those obtained by a marker based system.

DESCRIPTION OF RIGID BODY ORIENTATION IN THREE-DIMENSIONS

Several methods for representing the orientation between two body segments in three-dimensional space have been proposed (Goldstein, 1950; Chao, 1980; Grood & Suntay, 1983; Yeadon, 1990; Woltring, 1991; Cole et al., 1993). This section discusses some of these methods (Cole et al., 1993).

The position of a particle in three-dimensional space may be represented as a vector with three components, each representing one of the three translational degrees of freedom (DOF). The description of the position of a rigid body in three-dimensional space additionally requires information that describes its orientation in space. If a Cartesian coordinate system with axes, ξ'_i $(i = 1, 2, 3)$, is embedded in a rigid body, then the orientation of the rigid body (Figure 3.6.7) relative to a reference Cartesian coordinate system with axes, ξ_i $(i = 1, 2, 3)$, is defined by a 3×3 rotation matrix, [R], with components, $R_{ij} = \cos(\xi'_i, \xi_j)$ $(i, j = 1, 2, 3)$. This matrix is also referred to as the direction cosine matrix or attitude matrix, and it can be used as an operator to transform the components of a vector from one coordinate system to the other:

$$\{\xi'\} = [R]\{\xi\} \text{ and } \{\xi\} = [R]^{-1}\{\xi'\}$$

where $\{\xi\}$ and $\{\xi'\}$ are a common vector represented in the two systems. The rotation matrix has the properties that its inverse is equal to its transpose, $[R]^{-1} = [R]^T$, and its determinant is equal to one, $|R| = 1$. A detailed description of a least squares method for the determination of the rotation matrix from the coordinates of landmarks fixed to a body is given in Veldpaus et al. (1988).

For the interpretation of body segment orientation in biomechanical analyses, a parametric representation of the rotation matrix is usually desired. Current parametric representations include:

- Cardan/Euler angles,
- Joint Coordinate Systems (JCS),
- Finite helical axes and rotations, and
- Helical angles.

These parametric representations are discussed in this section, with emphasis given to Cardan/Euler angles and the JCS. The discussion is based on the following assumptions:

- Cartesian coordinate systems have been embedded in each body segment of interest, with the x-axis pointing anteriorly, the y axis vertically, and the z-axis to the right when the subject is in the anatomical position,
- The orientation of a body segment relative to an inertial reference system is specified by a rotation matrix, and
- The orientation of one body segment with respect to another, i.e., joint orientation, is specified by a rotation matrix.

Cardan/Euler angles

In the Cardan/Euler angle representation of three-dimensional orientation, the rotation matrix is parameterized in terms of *three independent angles,* resulting from an ordered sequence of rotations about the axes (i, j, k), of a selected Cartesian coordinate system (x_1, y_1, z_1), to obtain the attitude of a second coordinate system (x_2, y_2, z_2), relative to the first (Figure 3.6.10). When the first and the last axes are the same, (i = k), the term Euler an-

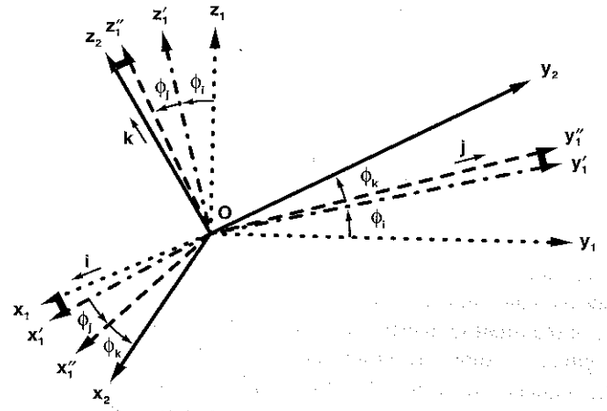

Figure 3.6.10 **Sequential rotations ϕ_i, ϕ_j, and ϕ_k about the axes i, j, and k from the starting coordinate system (x_1, y_1, z_1) to obtain the orientation of the second coordinate system (x_2, y_2, z_2). The axes i, j, and k have been arbitrarily defined as the x, y, and z axes, respectively, although they are not restricted to this definition.**

gles is used. When all three axes are different, the term Cardan angles is used, and it is this representation that is typically used in biomechanics (Woltring, 1991). When referring to other sources, caution must be used, because some investigators use the terms Cardan and Euler angles differently. The i and k axes correspond to axes in each of the two segment embedded coordinate systems, while the j axis is referred to as the nodal axis.

The parametric representation is mathematically defined by:

$$[R_{ijk}] = [R_k(\phi_k)][R_j(\phi_j)][R_i(\phi_i)]$$

where:

$[R_{ijk}]$ = parametric representation of the rotation matrix for the chosen sequence of rotations

$[R_i(\phi_i)]$ = parametric representation of the rotation matrix for a rotation, ϕ_i, around the specific axis i. An analogous definition is used for the rotations about the axes j and k

The parametric rotation matrices for rotations about the x, y, and z axes of a Cartesian coordinate system are defined as:

$$[R_x(\phi_x)] = \begin{bmatrix} 1 & 0 & 0 \\ 0 & \cos\phi_x & \sin\phi_x \\ 0 & -\sin\phi_x & \cos\phi_x \end{bmatrix}$$

$$[R_y(\phi_y)] = \begin{bmatrix} \cos\phi_y & 0 & -\sin\phi_y \\ 0 & 1 & 0 \\ \sin\phi_y & 0 & \cos\phi_y \end{bmatrix}$$

$$[R_z(\phi_z)] = \begin{bmatrix} \cos\phi_z & \sin\phi_z & 0 \\ -\sin\phi_z & \cos\phi_z & 0 \\ 0 & 0 & 1 \end{bmatrix}$$

Since matrix multiplication is not commutative, the final parametric rotation matrix, $[R_{ijk}]$, depends on which of the axes x, y or z is chosen for the rotations i, j, and k. The parameterization of the rotation matrix into Cardan angles, therefore, is *sequence dependent*. For a given segment or joint orientation, different component values can be obtained depending on the sequence selected. Once the rotational sequence has been determined, the parametric rotation matrix can be constructed in terms of the angles ϕ_x, ϕ_y, and ϕ_z. The resulting expressions can then be equated to the numerical values of the rotation matrix for the selected orientation to solve for each angle. For example, if the axes i, j, and k are arbitrarily defined as the axes z, y, and x, respectively, the parametric rotation matrix is constructed as:

$$[R_{zyx}] = [R_x(\phi_x)][R_y(\phi_y)][R_z(\phi_z)]$$

$$[R_{zyx}] = \begin{bmatrix} (C\phi_z C\phi_y) & (S\phi_z C\phi_y) & (-S\phi_y) \\ (-S\phi_z C\phi_x + C\phi_z S\phi_y S\phi_x) & (C\phi_z C\phi_x + S\phi_z S\phi_y S\phi_x) & (C\phi_y S\phi_x) \\ (S\phi_z S\phi_x + C\phi_z S\phi_y C\phi_x) & (-C\phi_z S\phi_x + S\phi_z S\phi_y C\phi_x) & (C\phi_y C\phi_x) \end{bmatrix}$$

where:

$S\phi_k = \sin\phi_k$

$C\phi_k = \cos\phi_k$

If the numerical components of the rotation matrix, [R], are labeled as, R_{mn} (m = 1, 2, 3; n = 1, 2, 3), and counter-clockwise rotations are chosen as positive, the sine and cosine of each angle can be calculated from:

$$\sin\phi_y = -R_{13} \qquad \cos\phi_y = \sqrt{1 - \sin^2\phi_y}$$

$$\sin\phi_x = \frac{R_{23}}{\cos\phi_y} \qquad \cos\phi_x = \frac{R_{33}}{\cos\phi_y}$$

$$\sin\phi_z = \frac{R_{12}}{\cos\phi_y} \qquad \cos\phi_z = \frac{R_{11}}{\cos\phi_y}$$

From these equations, each angle can be determined in the range, $-\pi < \phi < \pi$, so that the time history of the angle is continuous (Yeadon, 1990).

(i) Sequence selection in Cardan/Euler angles

The sensitivity of calculations of joint orientation to the rotational sequence is illustrated in Figure 3.6.11. The differences in component values, $\Delta\phi$, for two different sequences of ordered rotations were determined for the ankle joint complex, with the second and third rotations the reverse of those shown in the previous example. The results indicate that, theoretically, there are substantial differences in orientation components for different Cardanic sequences. However, the differences are not always relevant in practical applications to human movement. Differences in relative segmental orientations of the lower extremities in running due to different sequences of ordered rotations are minimal. However, in a side shuffle movement, with a larger in-eversion range-of-motion, the differences can be large. In range-of-motion (ROM) measurements, the differences are substantial, and results from different sequences of ordered rotations cannot be compared (Table 3.6.1). These sensitivity considerations illustrate the need for a well-defined convention for biomechanical analysis.

In biomechanics, the three Cardan angles are typically used to represent the anatomical components of joint orientation and movement, e.g., flexion-extension, adduction-abduction, and inversion-eversion. The anatomical components of movement are defined with respect to the anatomical position, as follows (Moore, 1980; Snell, 1973):

Flexion-extension is motion of a segment in a *parasagittal plane.*

Adduction-abduction is motion of a segment *away from or toward the sagittal plane.*

Axial rotation of a segment is rotation of a segment about its *longitudinal axis.* Note: the terminology of the third rotational component differs depending on the joint.

For practical use in biomechanics, the sequence of ordered rotations should be chosen so that the anatomical definitions are satisfied. Rotational sequences that do not conform to these definitions should be avoided. The following argument provides evidence that the sequence of Cardan angles that satisfies the definitions of flexion-extension, adduction-abduction, and third component rotation occurs in the following order:

Table 3.6.1 Comparative numerical results for measurements of angular positions for the ankle joint complex for running, side shuffle, and range of motion (ROM) positions (unpublished, Cole, 1992, with permission).

ACTIVITY	COMPONENT	ANGLE SEQUENCE PL-DO/AD-AB/IN-EV	ANGLE SEQUENCE PL-DO/IN-EV/AD-AB
RUNNING	DO	25	21.4
	AB	10	10.6
	EV	20	19.7
SIDE SHUFFLE	DO	20	30.3
	AB	15	18.1
	IN	35	33.6
ROM	PL	40	26.8
	AB	40	41.8
	IN	20	15.2

- Flexion-extension,
- Adduction-abduction, and
- Axial rotation.

The flexion-extension component, first in the sequence, must occur within the parasagittal plane. The second rotation must occur in a plane perpendicular to the sagittal plane since the coordinate system is orthogonal. Therefore, the second rotation satisfies the anatomical definition of adduction-abduction. Axial rotation is the third rotation in the sequence. After the first two rotations are completed, the remaining axis must correspond to the longitudinal axis of the distal segment, which again satisfies the anatomical definition for the final rotation. Consequently, the proposed sequence of (1) flexion-extension, (2) adduction-abduction, and (3) axial rotation conforms to the anatomical definitions of segment rotations.

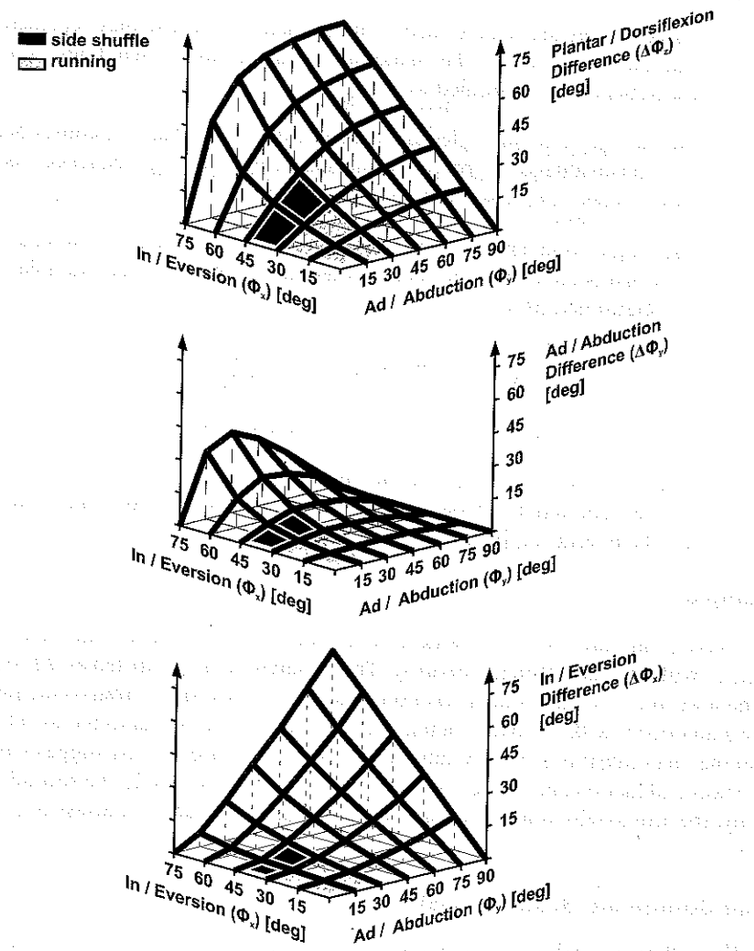

Figure 3.6.11 Differences in the calculated values for plantar-dorsiflexion (top), ad-abduction (centre), and in-eversion for two different sequences of rotation with the second and third rotation reversed. The primary sequence that is illustrated is plantar-dorsiflexion, ad-abduction, and in-eversion. ϕ_z was arbitrarily chosen as 45°. ϕ_x and ϕ_y were varied from 0° to 90° and the rotation matrices were generated based on the primary sequence. The representations of ϕ_x, ϕ_y, and ϕ_z in the secondary sequence were calculated from the generated rotation matrices and compared to the primary values (from Cole et al., 1993, with permission).

It can easily be demonstrated that the sequence (1) flexion-extension, (2) axial rotation, and (3) adduction-abduction does not satisfy the above anatomical definitions. If axial rotation is chosen as the second rotation, the third rotation no longer conforms to the definition of adduction-abduction, since it is not constrained to a plane perpendicular to the sagittal plane.

(ii) Advantages and disadvantages of Cardan angles

(1) Cardan angles are widely used in biomechanics, because they represent joint orientation analogous to the anatomical representation that both clinicians and researchers are accustomed to using.

(2) The fact that Cardan angles are sequence dependent has sometimes been viewed as a disadvantage. Appropriate standardization of the sequence, as proposed above, is one simple solution to this problem.

(3) One major disadvantage of Cardan angles is gimbal lock. A mathematical singularity that occurs when the second rotation equals $\pm \pi/2$. For example, ϕ_x and ϕ_z are determined from:

$$\sin\phi_x = \frac{R_{23}}{\cos\phi_y} \quad \text{and} \quad \sin\phi_z = \frac{R_{12}}{\cos\phi_y}$$

If $\phi_y = \pm\pi/2$, then ϕ_x and ϕ_z are undefined.

(4) Problems may result from the fact that finite rotations are not vector quantities. A simple subtraction of one orientation from another one can yield erroneous results in terms of the path of motion.

Example 1

Consider an initial position of the arm in which it is outstretched laterally, at 90° to the vertical, with the palm facing anteriorly. This orientation is quantified as 90° of abduction of the arm from the anatomical position. The arm is moved in a transverse plane until it points anteriorly with the palm facing up. This orientation is quantified as 90° of flexion from the anatomical position. A subtraction of the two orientations suggests that the arm underwent adduction and flexion in the movement from the first to the second position. In reality, the arm axially rotated while moving through a 90° arc in a transverse plane of the body.

Joint Coordinate System (JCS)

Three-dimensional joint orientation is interpreted as a set of three rotations that occur about the axes of a Joint Coordinate System (JCS) (Figure 3.6.12).

(1) One axis, with unit vector, $\mathbf{e}_1$, is selected to be the medio-lateral (z) axis of the proximal segment coordinate system. This is the rotational axis for flexion-extension at the joint.

(2) Another axis, with unit vector, $\mathbf{e}_3$, is selected to be the longitudinal axis of the distal segment. The axial rotation component is measured about this longitudinal axis of the distal segment.

(3) These two segment-fixed axes define the remaining axis, with mutually-perpendicular unit vector, $\mathbf{e}_2$. This remaining axis is the cross-product of the two segment-fixed axes, and it defines the axis of rotation for adduction-abduction at the joint.

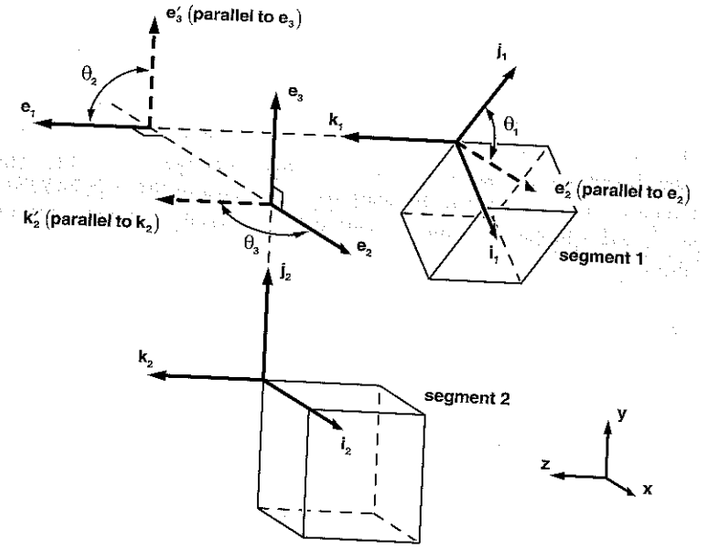

Figure 3.6.12 **Illustration for the definition of the Joint Coordinate System (JCS) (from Grood and Suntay, 1983, with permission).**

The equations for the JCS were originally presented for the specific application to the knee joint (Grood & Suntay, 1983). These equations are presented below in a modified form to make them applicable in the general case (Cole et al., 1993). The equations cannot be expressed in general terms using the coordinate axes x, y, and z. Depending on which axes are selected for the two segment-fixed axes, it is possible to obtain both a right- and left-handed Joint Coordinate System.

To ensure a right-handed Joint Coordinate System, an alternative labelling of segment-fixed coordinate axes is used:

F-axis — Flexion-extension axis. Chosen as the axis of the segment coordinate system that is oriented predominantly in the medio-lateral direction. The axis is described by the unit vector, **f**.

L-axis — Longitudinal axis. Chosen as the axis of the segment coordinate system that is oriented predominantly lengthwise along the distal segment. The axis is described by the unit vector, **l**.

T-axis — Third axis. Calculated as the cross-product of the longitudinal axis and the flexion-extension axis. The axis is defined by the unit vector, **t**, resulting from the cross-product:

$$\mathbf{t} = \mathbf{l} \times \mathbf{f}$$

where:

$\times$ = symbol for vector cross product

The unit vectors, **l**, **f**, and **t** are obtained from the rotation matrix that specifies the orientation of the segment of interest that is relative to an inertial reference system. As an illustration, if the flexion-extension axis is chosen as the z-axis, then, $\mathbf{f} = \{R_{31}, R_{32}, R_{33}\}$.

The unit vectors that describe the orientations of the axes of the JCS between a reference segment, i, and a target segment, j, relative to an inertial reference system are described as follows.

$$\mathbf{e}_{1_{ij}} = \mathbf{f}_i$$

$$\mathbf{e}_{2_{ij}} = \left(\frac{\mathbf{e}_{3_{ij}} \times \mathbf{e}_{1_{ij}}}{\left| \mathbf{e}_{3_{ij}} \times \mathbf{e}_{1_{ij}} \right|} \right) \cdot A$$

where:

$$A = \begin{cases} -1 \text{ if } & \left(\mathbf{e}_{3_{ij}} \times \mathbf{e}_{1_{ij}} \right) \bullet \mathbf{t}_j < 0 \\ & \text{and:} \\ +1 \text{ otherwise} & \left(\left(\mathbf{e}_{3_{ij}} \times \mathbf{e}_{1_{ij}} \right) \times \mathbf{e}_{3_{ij}} \right) \bullet \mathbf{f}_j > 0 \end{cases}$$

$\bullet$ = dot product

$\cdot$ = scalar multiplication

$\mathbf{e}_{3_{ij}} = \mathbf{l}_j$

The three angles that represent the three-dimensional orientation of the target segment, j, with respect to the reference segment, i, relative to a neutral position are calculated as follows.

For the angle of rotation about the axis for flexion-extension:

$$\phi_{1_{ij}} = \arccos(\mathbf{e}_{2_{ij}} \bullet \mathbf{t}_i) \cdot \text{sign}(\mathbf{e}_{2_{ij}} \bullet \mathbf{l}_i)$$

For the angle of rotation about the axis for adduction-abduction:

$$\phi_{2_{ij}} = \arccos(\mathbf{r} \bullet \mathbf{l}_j) \cdot \text{sign}(\mathbf{e}_{1_{ij}} \bullet \mathbf{e}_{3_{ij}})$$

where:

$$\mathbf{r} = \left(\frac{\mathbf{e}_{1_{ij}} \times \mathbf{e}_{2_{ij}}}{\left| \mathbf{e}_{1_{ij}} \times \mathbf{e}_{2_{ij}} \right|} \right)$$

For the angle of rotation about the axis for axial rotation:

$$\phi_{3_{ij}} = \arccos(\mathbf{e}_{2_{ij}} \bullet \mathbf{t}_j) \cdot \text{sign}(\mathbf{e}_{2_{ij}} \bullet \mathbf{f}_j)$$

where:

$$\text{sign}(x) = \begin{cases} 1 \text{ if } & x \geq 0 \\ -1 \text{ if } & x < 0 \end{cases}$$

Counter-clockwise rotations relative to the neutral position have been defined as positive. In comparison to the equations originally presented by Grood and Suntay (1983), the scalar, A, has been added to ensure that each of the three angles is continuous in the range, $-\pi < \phi < \pi$, and the unit vector, **r**, has been added to ensure that counter-clockwise rotations about the axis, $\mathbf{e}_2$, are always positive regardless of which axes are chosen for, $\mathbf{e}_1$ and $\mathbf{e}_3$.

A comparison of the JCS to the proposed sequence of Cardan angles shows the two parametric representations to be identical:

- The first body fixed axis, $\mathbf{e}_1$, corresponds to the first rotational axis of the Cardanic sequence,
- The axis, $\mathbf{e}_2$, corresponds to the nodal axis, and
- The second body fixed axis, $\mathbf{e}_3$, corresponds to the final rotational axis of the Cardanic sequence.

The three angles are calculated differently in the two methods. However, the principle remains the same and the results are identical.

(iii) Advantages and disadvantages of the JCS

(1) The advantages and disadvantages of the JCS for representing three-dimensional joint orientation are identical to those described for Cardan angles.

(2) The major difference between the JCS and the Cardan angle representation is conceptual. For a given joint orientation, the sequential nature of the Cardan angle approach implies that a movement from the neutral position is occurring to obtain the joint orientation of interest, which is not necessarily the case. The JCS, on the other hand, is conceptually an actual representation of a specific joint orientation. This difference would suggest that the JCS approach is the preferable one.

(3) The JCS can also be used to describe displacements. The Cardan and Euler angles only describe the relative orientation of two bodies. However, when using the JCS, the displacement can be described as three displacements, in turn, along each of the axes $\mathbf{e}_1$, $\mathbf{e}_2$, and $\mathbf{e}_3$.

Finite helical axis

Any finite movement of a body from a reference position can be described as a rotation about and a translation along a line in space (Woltring, 1991). This line in space is called the *finite helical axis*. To completely describe a movement, the following finite helical axis parameters must be specified:

n = the unit vector describing the orientation of the finite helical axis
s = a point on the helical axis, locating it in space
θ = the amount of rotation about the helical axis
d = the amount of translation along the helical axis

For any movement, the finite helical axis passes through the centre of rotation. For pure rotations, the finite helical axis is simply the axis of rotation, like the hinge of a door. If there are translations in the same plane as the rotations, then the axis can lie some distance from the body. If there are translations parallel to the axis, then the motion resembles that of a screw, and $d > 0$. The helical axis description of a movement can be awkward if there are translations with very small rotations. In cases like this, the location of the axis **s** can be very far from the body.

In addition to describing simply the relative orientations of two bodies, the finite helical axis provides information about how the displacement took place. When the movement of one body is described relative to a connected body, the finite helical axis can provide information about the joint between the two bodies. For any movements of the forearm with respect to the upper arm, for example, the helical axis will pass though the centre of the elbow joint and the direction of the rotation **n** will always be in the same direction, because the elbow joint is (for the most part) a revolute joint. For spherical joints, e.g., the hip joint, the axis will always pass through the centre of the hip, but the orientation can vary. For joints that are neither spherical nor revolute, the position and orientation of the helical axes can change. Helical axes can be used for describing the movement at joints because of information they provide about how the joint works.

The helical axis orientation parameters, **n**, θ, can be calculated from the rotation matrix for a selected angular displacement from one coordinate frame to the next. The axis position **s** and the translation d, can be determined from the displacement of the origin of the coordinate frame. The methods used to calculate the helical axis parameters in biomechanical applications are described in detail elsewhere, e.g., Spoor & Veldpaus (1980) and Woltring et al. (1985). In short, the helical axis can be found because for a given rotation and displacement, all points on the helical axis remain on the helical axis.

(iv) Advantages of finite helical axes

(1) When plotted relative to anatomical landmarks, finite helical axes provide a functional representation of the movement occurring at the joint, especially when the finite increments of rotation are chosen to be small.

(2) The finite helical axis approach provides information about the actual axes of rotation in a joint and linear translations of one body with respect to another, which cannot be obtained using Cardan or Euler angles.

(3) Finite helical axes do not suffer from gimbal lock. No orientations exist that cannot be represented by finite helical axes.

(v) Disadvantages of finite helical axes

(1) The finite helical axis does not provide a representation of joint orientation in terms of three anatomically and clinically meaningful parameters, as do Cardan angles and the JCS.

(2) Helical axis parameters are sensitive to noise in the spatial landmark coordinates, and to the magnitude of the finite rotation (Spoor, 1984; Woltring et al., 1985). However, the influence of the former can be substantially reduced with appropriate smoothing of the landmark coordinates (Woltring & Huiskes, 1985; Lange et al., 1990).

Helical angles

The concept of helical angles has been proposed as an alternative to Cardan or JCS angles (Woltring, 1991; Woltring, 1992). Helical angles are a condensation of the information included in finite helical axes, and only include the components involved in the change or difference in orientation (translations are not described). The three helical angles are calculated from the components of the finite helical axis:

$$\boldsymbol{\theta} = (\theta_x, \theta_y, \theta_z)^T = \theta\,\mathbf{n}$$

where:

n = unit direction vector of the finite helical axis (as above)

Helical angles have many of the same advantages (and disadvantages) as the finite helical axes. However, one advantage that they have over the helical axes is that they are as compact a description of orientation as Euler or Cardan angles (with only three parameters).

Helical angles (and finite helical axes) eliminate the problem of gimbal lock. Additionally, for rotations about a single coordinate axis, helical angles are the same as Cardan or JCS angles. As with Cardan or JCS angles, helical angles are not additive. However, they reduce the non-linear properties of the parametric representation of joint orientation (Woltring, 1991).

Final comments

The selection of the appropriate methodology for describing three-dimensional joint orientation must be determined by the application. Each approach has its own inherent advantages and disadvantages. The JCS approach, for example, produces a result that is easily understood in clinical and anatomical environments. The helical axis approach, on the other hand, provides results that better represent the functional movement that occurs at a joint.